Supporting Information

In situ lead oxysalts passivation layer for stable and efficient perovskite solar cells

Wenjing Hou[a*], Mengna Guo[a], Yunzhen Chang[a], Huan Bi[b*], Qing Shen[b], Yaoming Xiao[c], Gaoyi Han[a*]

[a] Institute of Molecular Science, Key Laboratory of Chemical Biology and Molecular Engineering of Education Ministry, Key Laboratory of Materials for Energy Conversion and Storage of Shanxi Province, State Key Laboratory of Quantum Optics and Quantum Optics Devices, Shanxi University, Taiyuan 030006, P. R. China.

[b] Faculty of Informatics and Engineering, The University of Electro-Communications, 1-5-1 Chofugaoka, Chofu, Tokyo 182-8585, Japan.

[c] College of Chemical Engineering and Materials Science, Quanzhou Normal University, Quanzhou 362000, P. R. China.

[*] Corresponding authors.

E-mail: houwenjing@sxu.edu.cn (Wenjing Hou); han_gaoyis@sxu.edu.cn (Gaoyi Han); hbi.trans.sci@gmail.com (Huan Bi)

Experimental Section

Material:

The ITO glass substrates were purchased from Jiangsu Yanchang Sunlaite New Energy Co., Ltd. The SnO_2 was bought from Alfa Aesar (tin (IV) oxide, 15% in H_2O colloidal dispersion). Rubidium iodide (RbI, 99.9%) was purchased from Aladdin. Cesium iodide (CsI, 99.99%), lead (II) iodide (PbI_2, 99.99%), lead (II) chloride ($PbCl_2$, 99.99%), and methylamine hydrochloride (MACl, 99.5%) were bought from Xi'an

Polymer Light Technology Corp. Advanced Election Technology CO., Ltd. Lead (II) bromide ($PbBr_2$, 99.9%), Formamidine hydroiodide (FAI, 99.9%), bis(trifluoromethane) sulfonimide lithium salt (Li-TFSI, 99%), 4-tert-butyl pyridine (tBP, 99%), and 2,2′,7,7′-Tetrakis[N,N-di(4-methoxyphenyl)amino]-9,9′-spirobiflu-Orene (Spiro-OMeTAD, 99.86%) and N,N-dimethylformamide (DMF, 99.8%), dimethyl sulfoxide (DMSO, 99.9 %), and chlorobenzene (CB, 99.8 %) were obtained from Sigma Aldrich. Shanghai Macklin Biochemical Co., Ltd. supplied rubidium sulfate (Rb_2SO_4, 99.0%).

***Device Fabrication*:**

The etched ITO glass was ultrasonically cleaned for 20 min using detergent, deionized water, and ethanol, sequentially. After being blown dry by nitrogen (99.99%), and then the ITO was treated for 30 min with ultraviolet ozone (UV-O_3). The SnO_2 colloidal solution was prepared by combining the SnO_2 solution with deionized water at a volume ratio of 1:3. The as-prepared SnO_2 colloidal solution was filtered by the 0.22 μm polytetrafluoroethylene (PTFE) filter before use. The SnO_2 colloidal solution was spin-coated onto clean ITO glass substrates in ambient air with a spin rate of 3000 rpm for 30 s and annealed on a hot plate at 150 °C for 30 min. Afterwards, SnO_2 films were treated by UV-O_3 for 20 min. The 1.55 M perovskite precursor solution was prepared by dissolving FAI of 248.16 mg, CsI of 19.73 mg, RbI of 6.58 mg, PbI_2 of 682.73 mg, $PbBr_2$ of 8.53 mg, $PbCl_2$ of 12.74 mg, and MACl of 35 mg in the mixed solvents of DMF and DMSO (V_{DMF} : V_{DMSO} = 4 : 1). Different concentrations of Rb_2SO_4 (0.0, 0.1, 0.2, and 0.3 mg/mL) was added into the as-prepared precursor solution. The as-prepared perovskite precursor solution was filtered by the filter before use. The perovskite films were prepared through spin-coating the perovskite precursor solution on the SnO_2 films at 4000 rpm for 30 s where 80 μL CB antisolvent was dripped on perovskite films at 17 s before ending the program. The films were subsequently annealed at 130 °C for 28 min. The Spiro-OMeTAD solution was prepared by mixing 72.3 mg Spiro-OMeTAD, 28.8 μL of 4-tert-butyl pyridine (*t*BP) and 17.5 μL of lithium bis(trifluoromethane) sulfonyl imide (Li-TFSI) stock solution (520 mg Li-TSFI in 1 mL acetonitrile) in 1 mL CB. The hole transport layer was then

formed by spin-coating 20 μL of Spiro-OMeTAD solution onto the perovskite films at 4000 rpm for 30 s. Finally, a about 100 nm gold counter electrode was thermally evaporated on the top of Spiro-OMeTAD film under a vacuum of 3×10^{-5} Pa through using a shadow mask. The control device is based on the perovskite precursor solution without adding Rb_2SO_4, and the target device is based on the perovskite precursor solution with Rb_2SO_4.

Characterization

J-*V* curves were generated using a solar simulator and a Keithley 2400 source meter and the size of the active area of the devices was defined to be 0.1 cm^2 by using a metal mask. The light intensity was calibrated using a light irradiation meter and a standard silicon solar cell. The *J-V* curves were measured from 0 V to 1.2 V (forward scan) or from 1.2 V to 0 V (reverse scan) with a scan rate of 100 mV s^{-1}. An FTIR spectrometer was used to acquire Fourier transformed infrared (FTIR) spectra (Tensor27, BRUKER, Germany). Thermo Avantage (v5.9921) software was used to analyze and interpret XPS spectra acquired from a Physical Electronics Model 5700 XPS equipment. SEM observations were carried out in ADD mode on SEM (FESEM, JEOL-JSM-6701F). An X-ray diffractometer (XRD) was used to characterize the crystallinity of the perovskite films (D2 PHASER Desktop XRD, BRUKER, Germany). Liquid Ultraviolet-visible (UV-vis) spectra were recorded on U-3900 UV-Visible spectrophotometer. The steady state photoluminescence (PL) curves were carried out using confocal raman systems (iHR 550 HORIBA) with laser of 532 nm. In Shanxi University's State Key Laboratory of Quantum Optics and Quantum Optics Devices, time-resolved photoluminescence (TRPL) was measured using a self-built scanning confocal system based on an inverted microscope (Nikon, TE2000-U) with a 450 nm laser. The external quantum efficiencies (EQE, Zennium CIMPS-pcs2 (Zahner)) was measured with the tunable light source (TLS03). Impedance spectroscopy measurement was performed on an electrochemical workstation (China). The HR-TEM measurement was carried out on a high-resolution transmission electron microscope in high-resolution mode.

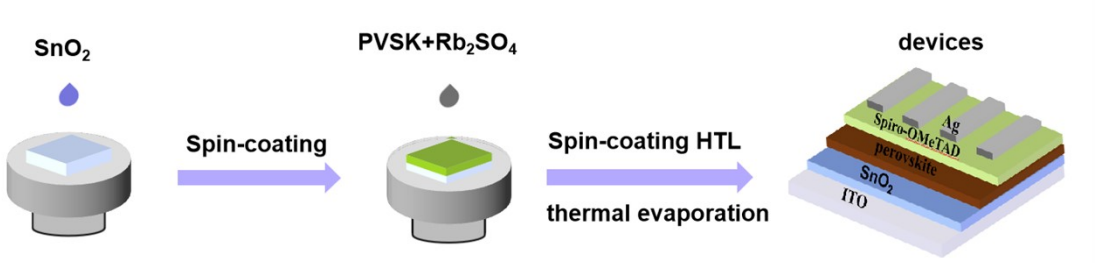

Fig. S1 The preparation process of perovskite solar cells.

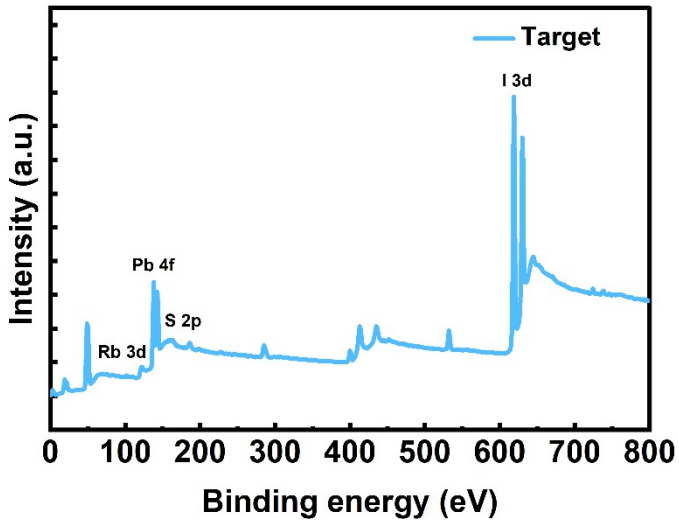

Fig. S2 The full XPS spectra of the perovskite film with Rb_2SO_4 additive.

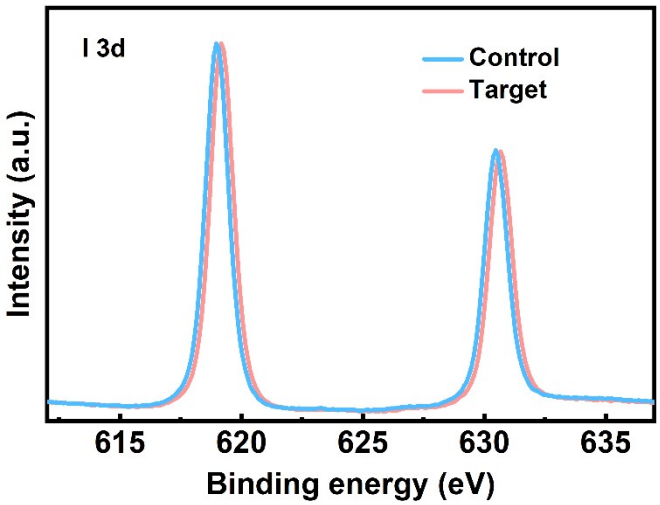

Fig. S3 I 3d for control and target perovskite films.

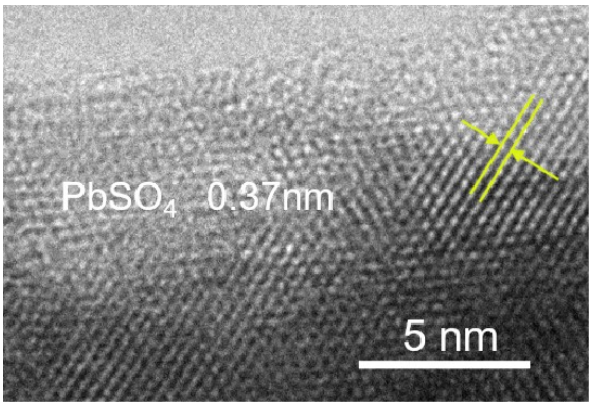

Fig. S4 TEM image of the perovskite precursor solution with Rb_2SO_4 additive.

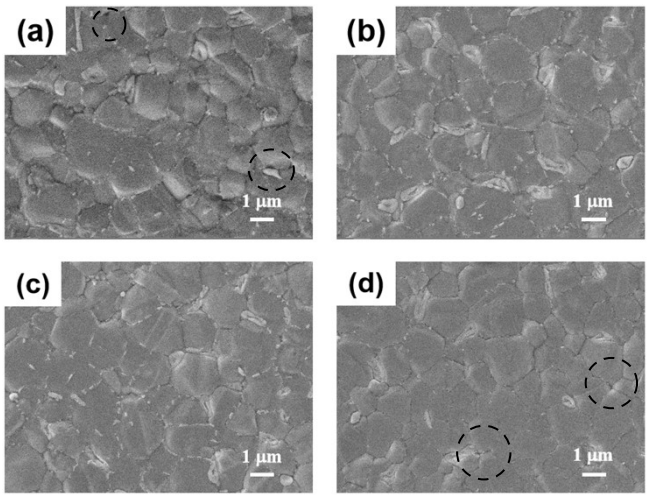

Fig. S5 Top-view SEM images of the perovskite films with different concentration of Rb_2SO_4 additive: (a) 0.00 mg/mL, (b) 0.10 mg/mL, (c) 0.20 mg/mL, and (d) 0.30 mg/mL, respectively.

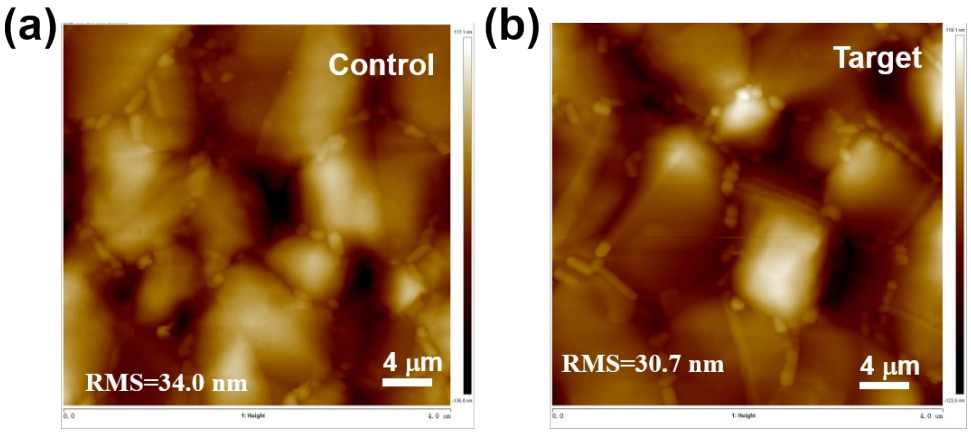

Fig. S6 AFM images of perovskite films (a) without and (b) with Rb_2SO_4 additive.

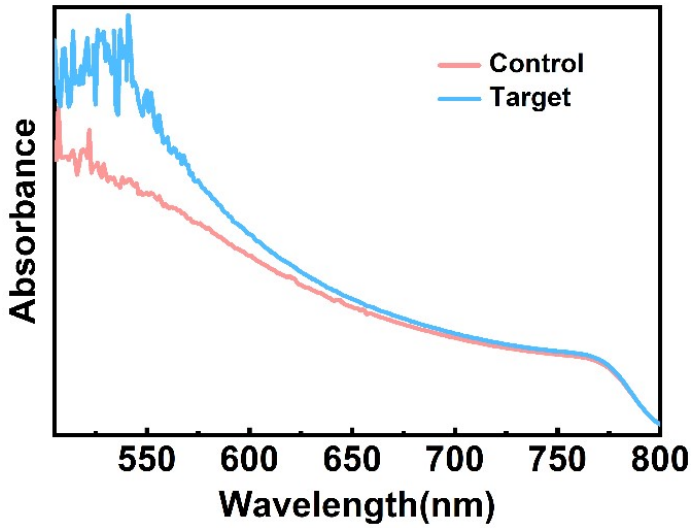

Fig. S7 UV-visible absorption spectra of perovskite films without and with Rb_2SO_4 additive.

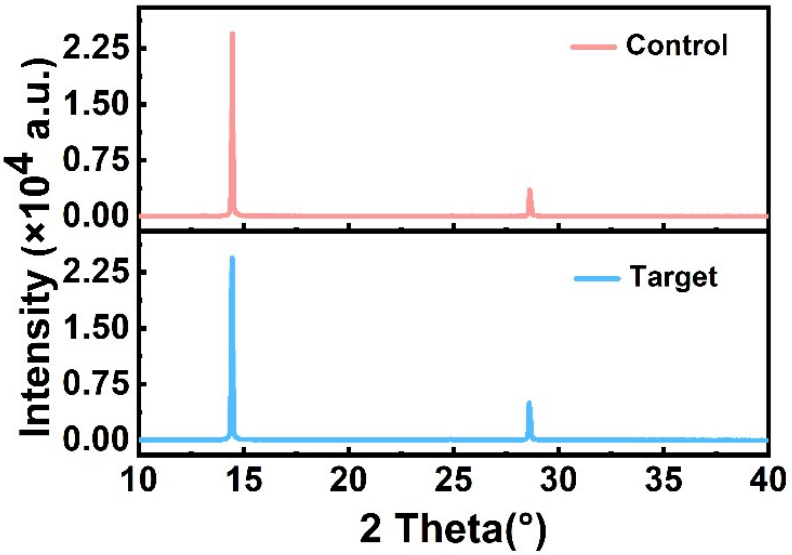

Fig. S8 XRD patterns of perovskite films without and with Rb_2SO_4 additive.

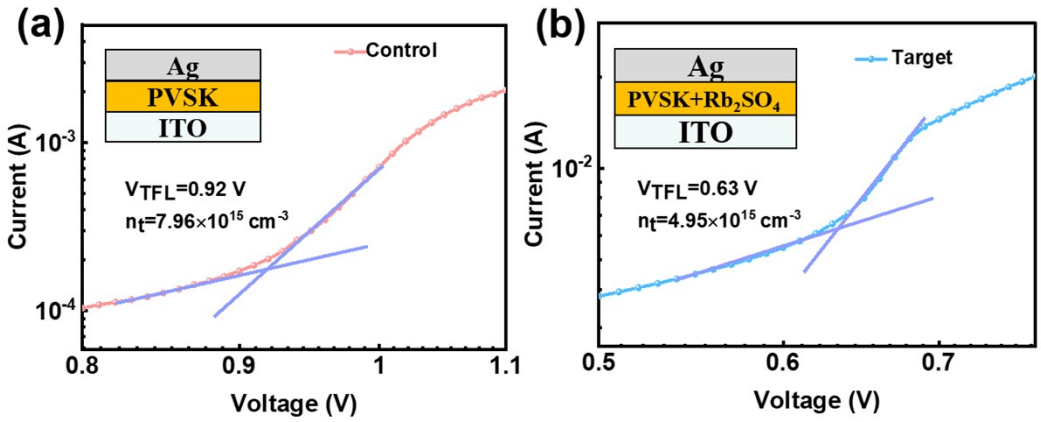

Fig. S9 The space charge limited current curves of the control and target devices.

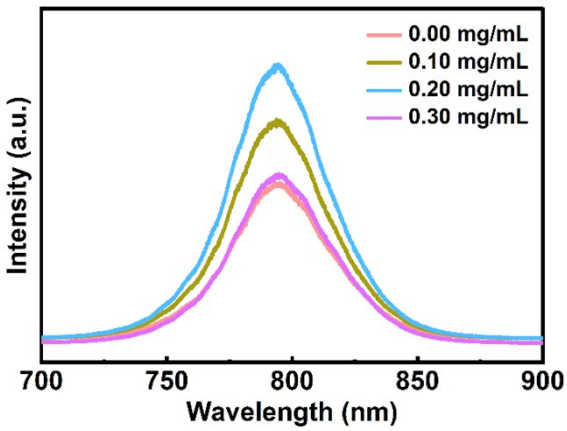

Fig. S10 Steady-state PL spectra of the perovskite films with different concentration of Rb_2SO_4 additive: 0.00 mg/mL, 0.10 mg/mL, 0.20 mg/mL, and 0.30 mg/mL, respectively.

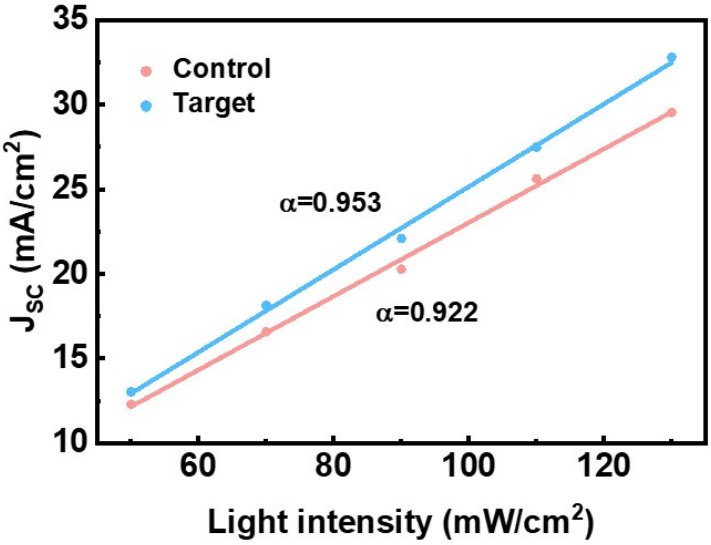

Fig. S11 J_{SC} dependence on light intensity for the control and target devices.

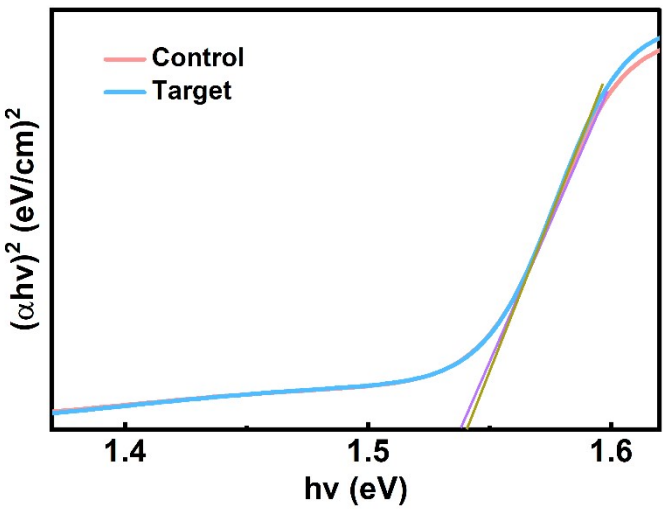

Fig. S12 Tauc plot of perovskite films.

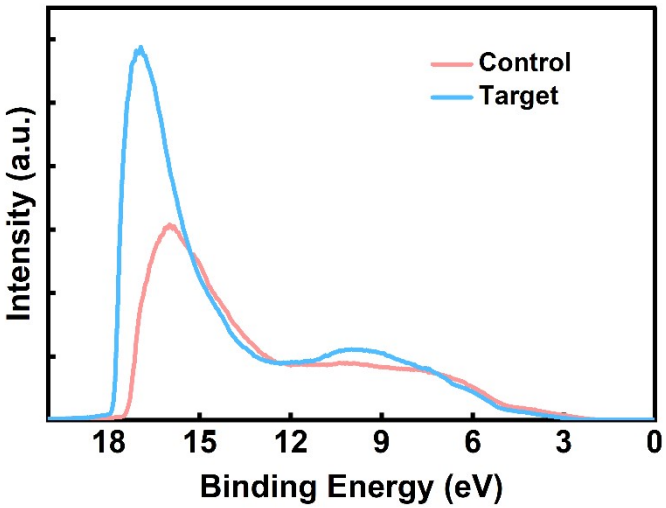

Fig. S13 Ultraviolet Photoelectron Spectroscopy of the perovskite films.

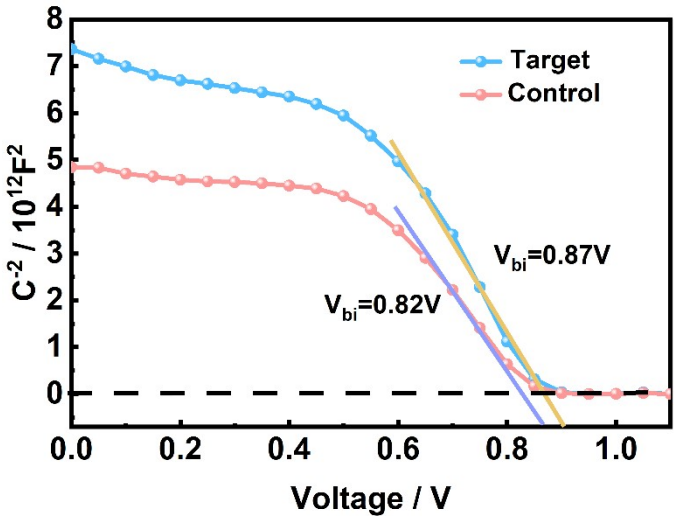

Fig. S14 Mott–Schottky curves of the control and target devices.

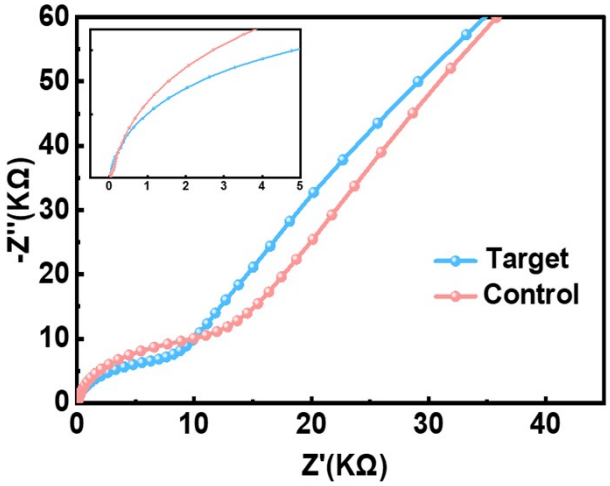

Fig. S15 Nyquist plots for the control and target devices.

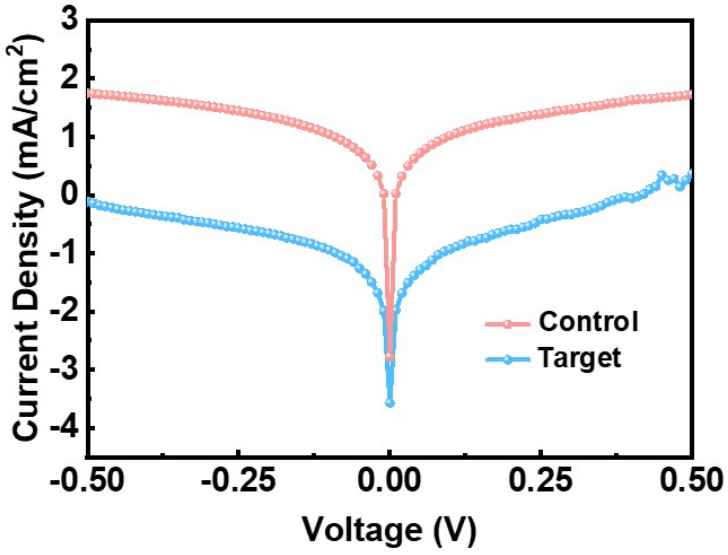

Fig. S16 *J* - *V* curves for the control and target devices in the dark condition.

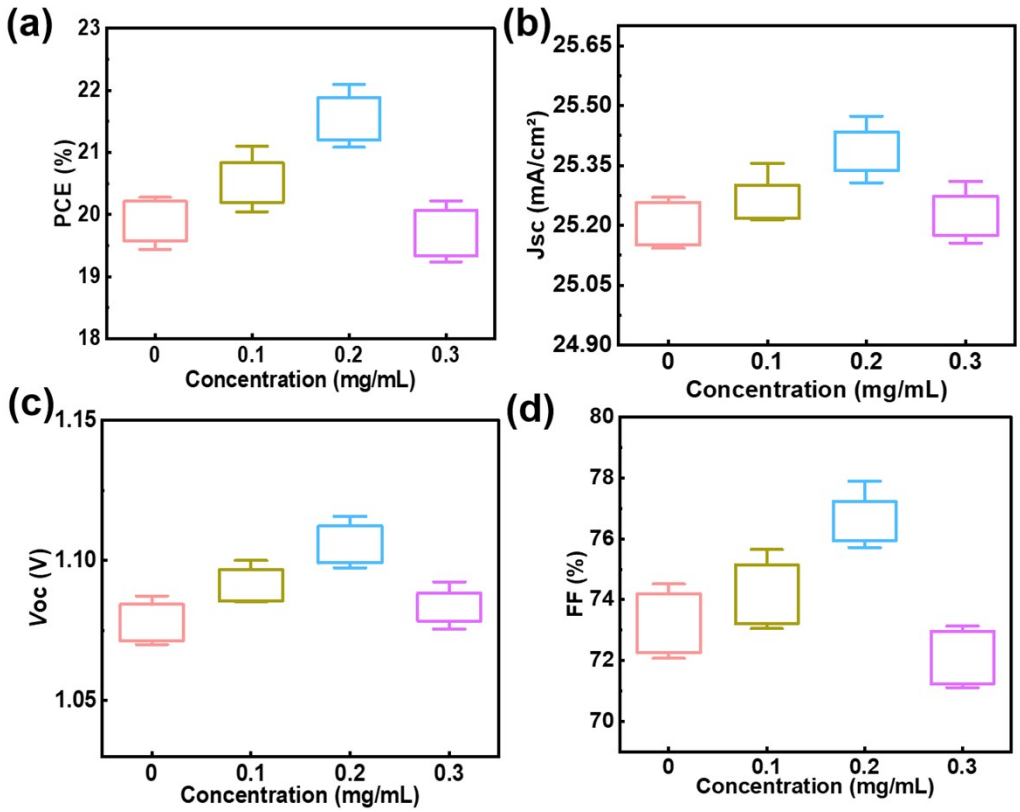

Fig. S17 Box charts of a) PCE, b) *J*sc, c) *V*oc and d) FF of the PSCs with different concentrations of Rb_2SO_4 additive.

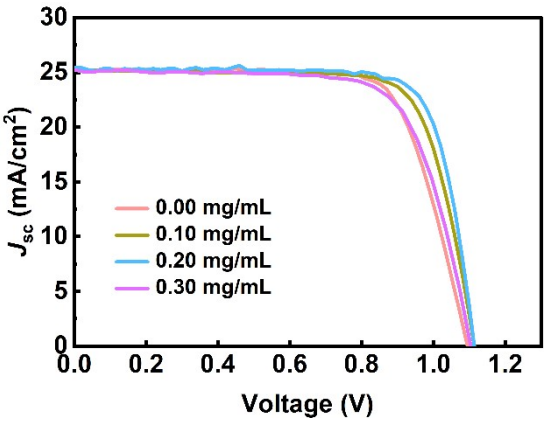

Fig. S18 The *J-V* curves of PSCs with different concentrations of Rb_2SO_4 additive.

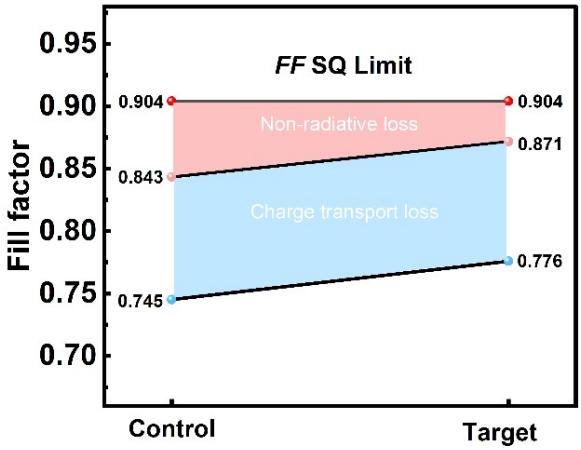

Fig. S19 The *FF* loss of devices, where blue, pink, res balls correspondingly represent the measured *FF*, FF_0 (without charge transport loss) and $FF_{S\text{-}Q.}$

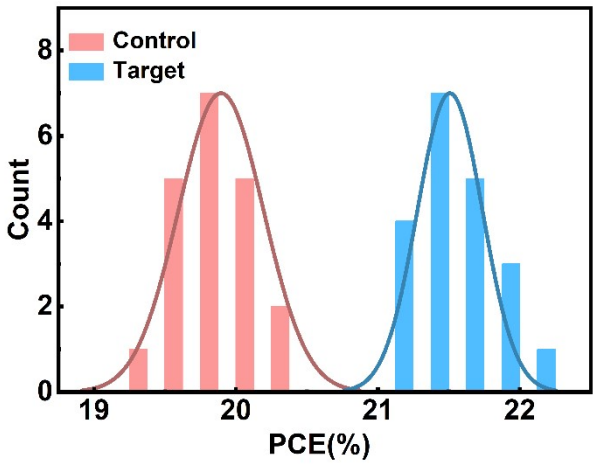

Fig. S20 Statistical histogram of PCEs of corresponding devices.

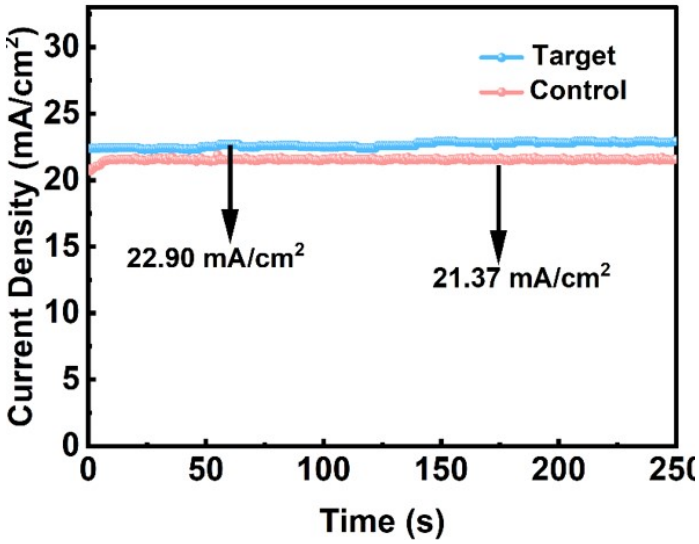

Fig. S21 The steady-state current density at the maximum power point for the control and target devices.

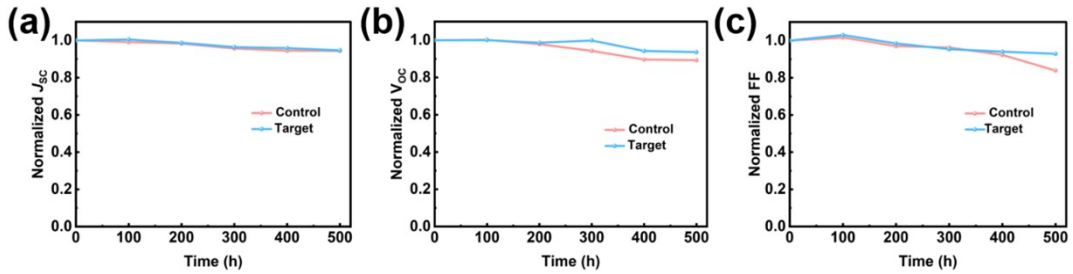

Fig. S22 a) J_{SC}, b) V_{OC}, and c) FF versus time for the unencapsulated control and target devices aged in the air with relative humidity of 15 %-20 % RH in the dark at the room temperature.

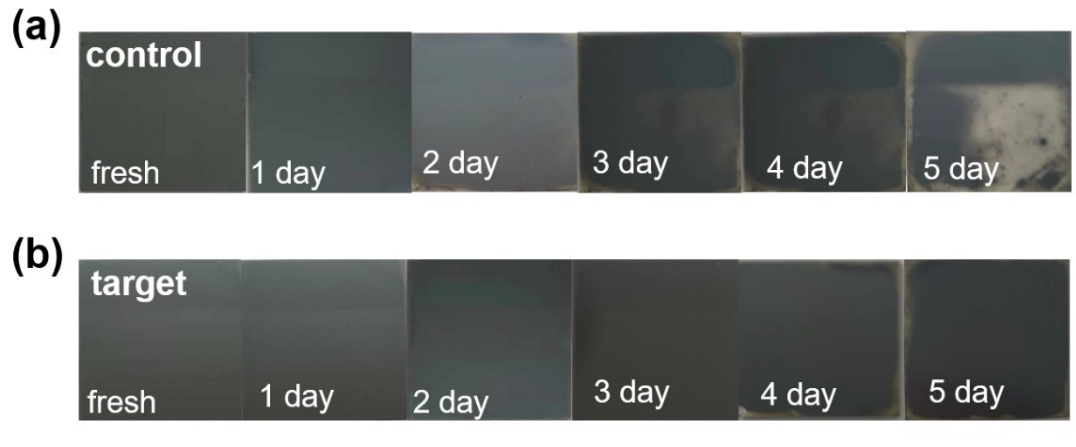

Fig. S23 Moisture stability of the perovskite films a) without and b) with Rb_2SO_4 exposed to a relative humidity of 50 %-60 % RH at the room temperature.

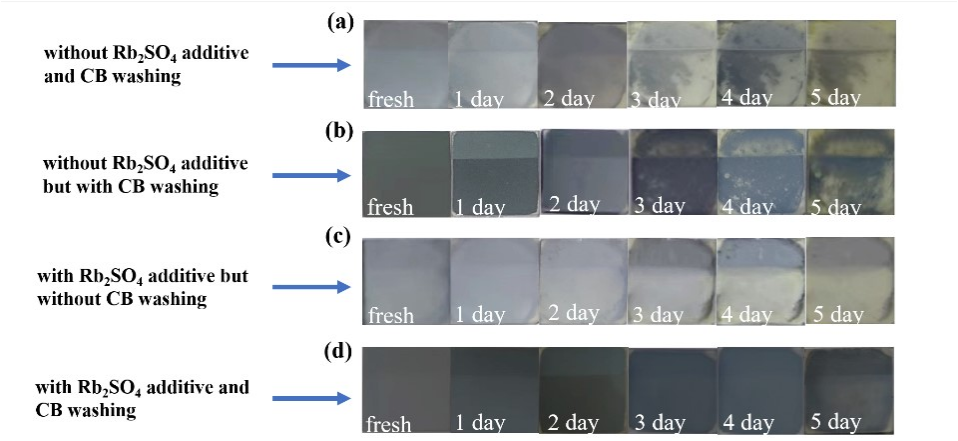

Fig. S24 Moisture stability of the perovskite films with different preparation condition exposed to a relative humidity of 60 ± 5% RH at the room temperature.

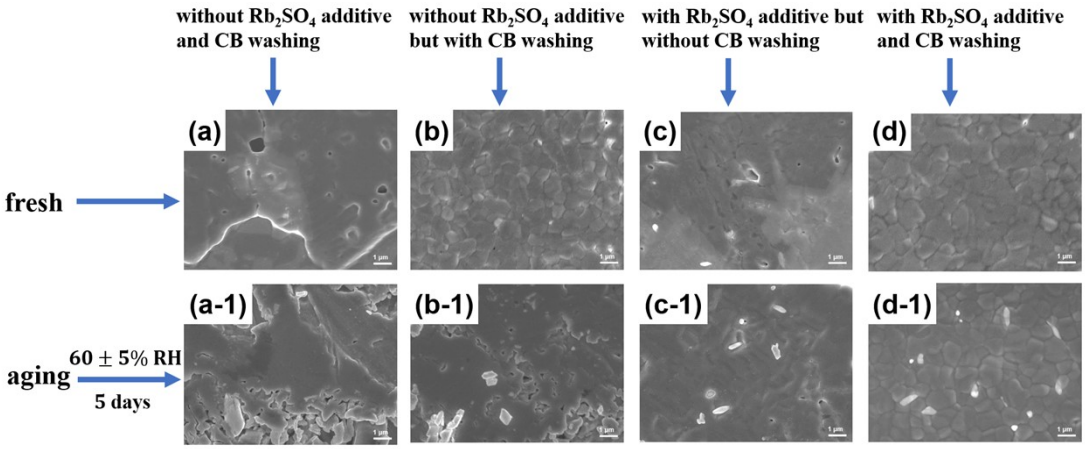

Fig. S25 Top-view SEM images of the perovskite films before and after aging.

Table S1. TRPL data of perovskite films perovskite films without with Rb_2SO_4 additive.

Sample	τ_1 (ns)	A_1 (%)	τ_2 (ns)	A_2 (%)	τ_{ave} (ns)
Control	19.51	0.833	119.53	0.167	75.40
Target	38.56	0.724	177.75	0.276	127.51

Table S2. Energy level parameters of materials used in the device.

Sample	E_{cutoff} (eV)	$E_{F, edge}$ (eV)	E_{VB} (eV)	E_g (eV)	E_{CB} (eV)
Control	17.69	1.91	-5.42	1.537	-3.88
Target	17.91	2.01	-5.30	1.540	-3.76

Table S3. Summary of the photovoltaic parameters of the PSCs with different concentrations of Rb_2SO_4 additive.

Rb_2SO_4 (mg/mL)	J_{sc} (mA cm^{-2})	V_{oc} (V)	*FF* (%)	PCE (%)
0.00	25.27	1.07	74.52	20.15
0.10	25.38	1.10	75.32	21.03
0.20	25.43	1.12	77.59	22.10
0.30	25.32	1.09	73.33	20.24

Table S4. Photovoltaic performances parameters of the control and target devices measured in reverse and forward scan under AM 1.5 G 1 sun illumination of 100 mW cm^{-2}.

Device	Scan	*J*sc (mA cm^{-2})	*V*oc (V)	FF (%)	PCE (%)	HI
Control	Forward	25.06	1.08	76.17	20.62	0.0225
	Reverse	25.27	1.07	74.52	20.15	
Target	Forward	25.39	1.11	78.95	22.25	0.0067
	Reverse	25.43	1.12	77.59	22.10	

Table S5. Average performances parameters of the 20 devices without and with Rb_2SO_4 modification measured in reverse scan.

Device	J_{SC} (mA cm^{-2})	V_{OC} (V)	FF (%)	*PCE* (%)
Control	25.17±0.15	1.08±0.02	73.22±1.30	19.90±0.57
Target	25.35±0.12	1.10±0.01	76.71±1.25	21.52±0.60